The current issue and full text archive of this journal is available at
www.emeraldinsight.com/0961-5539.htm

Natural convection in partially porous media: a brief overview

Dominique Gobin and Benoit Goyeau
Lab FAST, CNRS, Université Pierre et Marie Curie, Orsay, France

Received 5 December 2006
Revised 25 May 2007
Accepted 25 May 2007

Abstract

Purpose – This paper aims to provide a limited, but selective bibliography on modelling heat and mass transfer in composite fluid-porous domains.

Design/methodology/approach – Since the pioneer study by Beavers and Joseph, the problem of interface continuity and/or jump conditions at a fluid-porous interface has been of interest to the fluid mechanics and heat and mass transfer community. The paper is concerned both with numerical simulations of heat and fluid flow in such systems, and with the linear stability problems.

Findings – The one- and two-domain formulations are equivalent. Using the Darcy-Brinkman extension instead of the Darcy model reduces the number of *ad hoc* parameters in this configuration.

Research limitations/implications – The problem of double diffusive convection has still to be solved and analyzed.

Practical implications – The discussion on the interface conditions is of great relevance to many industrial and practical situations.

Originality/value – The important question of the macroscopic formulation of the problem is tackled in the paper.

Keywords Heat transfer, Modelling, Composite materials

Paper type General review

Nomenclature

A	= aspect ratio of the vertical enclosure (Section 3), H/L	H	= height of the enclosure, or thickness of the homogeneous porous layer m
C	= solute mass fraction, %wt	$\hat{H}$	= dimensionless height of the channel, H/h
C_P	= specific heat, J/kg K	$\mathbf{k}$	= unit vector (vertical direction)
$\mathscr{D}$	= mass diffusivity of the solute, m^2/s	k	= thermal conductivity, W/(m K)
d_f^*	= thickness of the fluid layer (m)	K	= permeability (m^2)
d_m^*	= thickness of the porous layer (m)	L	= width of the enclosure, m
d^*	= total thickness, $d^* = d_f^* + d_m^*$ (m)	Le	= Lewis number: α_f/D
$\hat{d}$	= thickness ratio of the horizontal layer (Section 4), d_f^*/d_m^*	N	= buoyancy ratio: $\beta_C \Delta C/\beta_T \Delta T$
Da	= Darcy number, K/H^2	$Nu(Sh)$	= average Nusselt (Sherwood) number $\int_0^1 -(\partial\theta/\partial x)\mathrm{d}z\left(\int_0^1 -(\partial\phi/\partial x)\mathrm{d}z\right)$
$\mathbf{g}$	= gravity vector, m/s^2	P	= dimensionless pressure

This study has been partially performed within the framework of an International Scientific Cooperation Program (PICS) between CNRS (France) and CNPq (Brazil). The calculations have been performed on the NEC-SX5 vectorial computer of IDRIS (CNRS-Orsay) with the support of the Engineering Division of CNRS (SPI) under grant No. 0336. Regular exchanges with Magda Carr (University of Dundee, UK) are gratefully acknowledged. The authors wish to thank Adrian Neculae, Silvia Hirata and Magda Carr for their contributions to this study.

International Journal of Numerical Methods for Heat & Fluid Flow
Vol. 18 No. 3/4, 2008
pp. 465-490
© Emerald Group Publishing Limited
0961-5539
DOI 10.1108/09615530810853682

Pr = Prandtl number, ν/α_f
Ra_T = thermal Rayleigh number, $g\beta_T\Delta TH^3/\alpha_f\nu$
Ra_T^* = Rayleigh number = $Gr_T PrDa$
T = dimensional temperature, K
$\mathbf{V}^*$ = dimensional fluid velocity (m/s)
V = dimensionless fluid velocity (V^*H/α_f)
V_m^* = dimensional filtration velocity
$w(u)$ = vertical (horizontal) component of V
x_P^* = dimensional width of the porous layer, m
x_P = dimensionless width of the porous layer, (x_P^*/L)
$x(z)$ = dimensionless coordinates, $x^*/H(z^*/H)$

Greek symbols

α_f = fluid thermal diffusivity, m^2/s
α_m = thermal diffusivity of the porous medium, m^2/s
α = slip coefficient of the Beavers and Joseph model
β = stress jump coefficient
β_T = thermal expansion coefficient: $-1/\rho_0(\partial\rho/\partial T)$
β_C = solutal expansion coefficient: $-1/\rho_0(\partial\rho/\partial C)$
γ_S = solid fraction
ΔC = concentration difference
ΔT = temperature difference
ε = porosity of the porous layer
ε_T = thermal diffusivity ratio, $\varepsilon_T = \alpha_f/\alpha_m$
κ = dimensionless wave number
μ_f = dynamic fluid viscosity, $kgm^{-1}s^{-1}$
μ_{eff} = effective dynamic fluid viscosity, $kgm^{-1}s^{-1}$
ν = kinematic viscosity, m^2/s
ψ = stream function: $u = -\partial\psi/\partial z$; $w = \partial\psi/\partial x$
ϕ = dimensionless concentration, $\phi = (C - C_0)/\Delta C$
ρ = fluid density, kgm^{-3}
σ = dimensionless complex growth rate of the perturbation $\xi = 1/\sqrt{Da}$
θ = dimensionless temperature, $\theta = (T - T_0)/\Delta T$
Θ = temperature perturbation

1. Introduction

Transport phenomena in composite domains consisting of a porous layer exchanging momentum, heat and/or constituents with an adjacent fluid are encountered in a wide range of industrial applications (thermal insulation, filtration processes, dendritic solidification, storage of nuclear waste, drying processes, spreading on porous substrates, ...) or in the context of environmental problems (geothermal systems, benthic boundary layers, ground-water pollution, ...).

This presentation deals more specifically with problems of natural convection in cavities or layers partially filled with a saturated porous medium. Following the pioneering study by Beavers and Joseph (1967), the model for fluid flow and heat and mass transfer in such media has to be analyzed in detail. We discuss the various alternatives proposed in the literature to assess the conservation equations in such domains. Depending on the fields of applications (insulation problems, solidification processes, pollution of aquifers, petrol engineering, ...), two approaches have been developed. On one hand, a two-domain formulation which considers the porous medium and the fluid as two distinct domains separated by a thin interface, where specific boundary conditions have to be explicitly written. On the other hand, a one-domain formulation combining the terms for the porous and the fluid domains in a set of generalized conservation equations valid for both domains. The transition from the porous to the fluid domain is defined by the spatial variation of the thermophysical properties. In the second section of the paper, fluid flow and heat and mass transfer due to double diffusion in a vertical enclosure is analyzed, and the influence of the presence of an even very thin porous layer is shown. Finally, both

formulations are compared in the case of the stability problem in an horizontal layer, where the fluid layer is on top of the porous medium.

2. One-domain vs two-domain formulation

The underlying modelling problem lies in the coupling between conservation equations in both regions and thus in the definition of appropriate boundary conditions at the fluid/porous interface. An accurate description of the convective heat or species transfer involved in the above-mentioned processes depends on the relevance of the momentum transport model at the interface. Owing to its theoretical and practical interest, the question of transport in porous media has been the subject of an intense research activity, reviewed in general books (Kaviany, 1995; Nield and Bejan, 2006). The two different approaches generally proposed to deal with this problem are discussed in the present section.

2.1 The two-domain approach

The majority of early studies dedicated to flow in fluid/porous configurations have dealt with the calculation of the drag force exerted by a fluid on a porous sphere (Joseph and Tao, 1966). The study by Beavers and Joseph (1967) assesses the problem of fluid flow in a rectangular channel including a porous layer, bringing special attention to the boundary condition at the fluid/porous interface. The forced flow in the channel (Figure 1) is described by the Stokes equation in the fluid and the momentum equation in the homogeneous porous layer by the Darcy law. These partial differential equations are of a different order and a slip boundary condition is proposed at the interface:

$$\left.\frac{\partial u^*}{\partial y^*}\right|_{y^*=0} = \frac{\alpha}{K^{1/2}}(u^*(0) - U^*(-H)) \tag{1}$$

where $u^*(y^*)$ is the velocity in the fluid channel, U^* the seepage velocity in the porous medium, K the permeability of the porous medium and α an empirical dimensionless

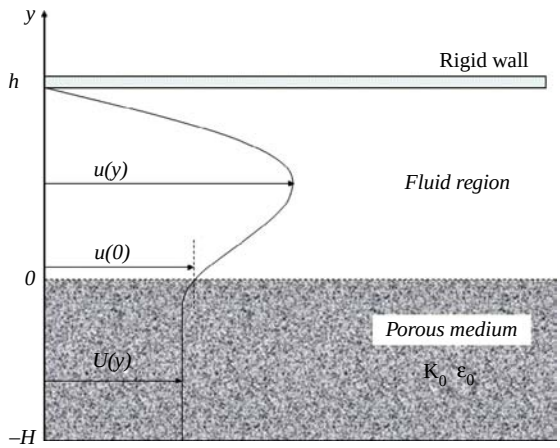

Figure 1.
Poiseuille flow in a fluid/porous channel

slip coefficient. A theoretical justification of condition (1) is given by Saffman (1971) using a statistical approach and a boundary layer approximation.

In this approach, $u^*(0)$ is found to be very sensitive to the exact location of the interface which is an unknown of the problem (Saleh *et al.*, 1993). This dependence has been numerically quantified by examining the axial and transverse flows near the surface of 2D periodic porous media (Larson and Higdon, 1986; Larson and Higdon, 1987). Several studies have focused on the determination of the slip parameter α which has been found to be strongly dependent on the local geometry of the interface (Beavers *et al.*, 1970; Taylor, 1971; Richardson, 1971) but not on the nature of the fluid (Beavers *et al.*, 1974). The experimental data provided by Beavers and Joseph (1967) are in good agreement with the analytical solution, but it has been necessary to adjust the value of α between 0.1 and 4 depending on the nature of the porous layer. This rather wide α range shows the important role of the porous structure at the interface even for materials having roughly the same macroscopic average properties in the core (Jäger and Mikelić 2000).

An alternative model consists in using the Brinkman equation in the porous layer (Brinkman, 1947; Neale and Nader, 1974):

$$0 = -\nabla P^* + \rho_f g - \mu_f K^{-1}\mathbf{V}^* + \mu_{eff}\nabla^2\mathbf{V}^* \tag{2}$$

where μ_{eff} is the effective viscosity of the porous medium and $\mathbf{V}^*$ is the dimensional filtration velocity vector. As the Stokes and Brinkman equations are of the same order, continuity of both stress and velocity can be satisfied at the interface. The analytical solution in the bulk fluid is then similar to the solution by Beavers and Joseph (BJ) provided that $\alpha = (\mu_{eff}/\mu_f)^{1/2}$. Equation (1) then becomes:

$$\left.\frac{\partial u^*}{\partial y^*}\right|_{y^*=0} = \sqrt{\frac{\mu_{eff}/\mu_f}{K}}(u^*(0) - U^*(-H)) \tag{3}$$

This formulation accounts for momentum transport in the porous layer at a thickness δ estimated to be on the order of $K^{1/2}$. The validity of Brinkman equation has been the subject of a controversial literature (Lundgren, 1972; Levy, 1981; Nield, 1983, 1991; Vafai and Kim, 1990, 1995) which it is not relevant to detail here. Let us only recall two main limitations: first, the Brinkman correction is significant only at high porosities, secondly the effective viscosity, which depends on the structure of the porous material, may strongly differ from the viscosity of the fluid. Although this latter aspect may be important, only a few studies over the last 30 years have been devoted to the determination of the effective viscosity (Larson and Higdon, 1987; Lundgren, 1972; Adler, 1978; Koplik *et al.*, 1983; Martys *et al.*, 1994; Givler and Altobelli, 1994). Most of them concern sparse porous structures or dilute suspensions where the reduced viscosity is found to be close to Einstein's (1906) law: $\mu_{eff}/\mu_f = 1 + 2.5\gamma_S$ where γ_S is the solid volume fraction. For denser beds of spheres and suspensions, according to Saffman (1971) and Lundgren (1972), the friction term does not only depend on the velocity but also on its first derivative and the comparison with the Stokes term allows for the determination of the effective viscosity, which is given by $\mu_{eff}/\mu_f = 1/(1 - 2.5\gamma_S)$ for moderately dense suspensions. The evolution shows a rapid decrease for $\gamma_S \geq 0.3$ in a "dense" bed of spheres, attributed to the interactions between particles that are not correctly described for dense systems. On the contrary,

recent numerical calculations for relatively dense systems ($0.2 \leq \gamma_S \leq 0.5$) show the monotonic behavior of the effective viscosity (Martys *et al.*, 1994). The influence of the flow through the Reynolds number also has been analyzed (Givler and Altobelli, 1994; Sahraoui and Kaviany, 1992). The derivation of a correct law for the effective viscosity is still under investigation (Starov and Zhdanov, 2001) and it probably depends on the tortuosity of the medium (Bear and Bachmat, 1990).

If we now consider the stress boundary condition, the model proposed by Ochoa-Tapia and Whitaker (1995a, b) introduces an interfacial jump condition based on the non-local form of the volume averaged Stokes's equation:

$$\mu_f \left.\frac{\partial u^*}{\partial y^*}\right|_{y^*=0} - \mu_{eff} \left.\frac{\partial U^*}{\partial y^*}\right|_{y^*=0} = -\frac{\beta}{\sqrt{K}}\, u^*(0) \tag{4}$$

where β is an adjustable parameter which must be experimentally determined (Ochoa-Tapia and Whitaker, 1995a). This description assumes that the porous layer is homogeneous, and comparing condition (4) to (3), it may be written:

$$\left.\frac{\partial u^*}{\partial y^*}\right|_{y^*=0} = \sqrt{\frac{\mu_{eff}/\mu_f}{K}}(u^*(0) - U^*(-H)) - \frac{\beta}{\sqrt{K}}\, u^*(0) \tag{5}$$

The analytical solutions of this model are in good agreement with the experimental results of BJ for β on the order of one. Unfortunately, no explicit dependence on the geometry of the interface is provided. Actually, condition (4) is an equivalent representation of the spatial variations of the porous structure at the interface (Goyeau *et al.*, 2003). Such a stress jump condition (4) may be used when inertia is significant (Kuznetsov, 1997) or for a Couette flow in a composite channel (Kuznetsov, 1998).

Among the numerical studies describing the interfacial flow, James and Davis (2001) use a singularity method to solve the flow field at the interface of a fibrous porous medium. For very large values of the porosity (greater than 0.9) their analysis mainly focuses on the slip velocity for both shear- and pressure-driven flows. In both cases, it is found that the Brinkman model strongly overestimates the flow penetration and the slip velocity (James and Davis, 2001).

2.2 The single-domain approach

In this approach, the porous layer is considered as a pseudo-fluid and the composite region is treated as a continuum. The transition from the fluid to the porous medium is achieved through a continuous spatial variation of properties, such as the permeability in the Darcy term of the modified Navier-Stokes equations (Arquis and Caltagirone, 1984; Beckermann *et al.*, 1987a, 1988). If the porous layer is assumed to be homogeneous, this equation takes the form:

$$\varepsilon^{-1}\frac{\partial}{\partial t}(\rho_f \mathbf{V}^*) + \varepsilon^{-2}\nabla.(\rho_f \mathbf{V}^*\mathbf{V}^*) = -\nabla P^* + \rho_f g - \mu_f K^{-1}\mathbf{V}^* + \mu_{eff}\nabla^2\mathbf{V}^* \tag{6}$$

where ε is the local porosity of the domain and $\mathbf{V}^*$ is the dimensional velocity vector. In the liquid channel, $\varepsilon = 1$, $\mu_{eff} = \mu_f$ and the permeability is infinite, so that the Darcy term is equal to zero and equation (6) reduces to the Navier-Stokes equation. In the homogeneous porous medium, ε is the bulk porosity and the effective viscosity value is given by the

corresponding relations. Note that for finite values of the permeability, all the terms involving the velocity are formally retained but the Darcy's term is predominant.

Since, this formulation avoids the explicit formulation of the boundary conditions at the fluid/porous interface, it has been extensively used in numerical computations dealing with thermal natural convection (Beckermann *et al.*, 1988; Turki and Lauriat, 1990; Lebreton *et al.*, 1991; Ettefagh *et al.*, 1991; Kuznetsov and Ming-Xiong, 1999; Mercier *et al.*, 2002) or double diffusive convection (Gobin *et al.*, 1998; Gobin *et al.*, 2005). A good agreement has been obtained in the comparison with experimental results (Beckermann *et al.*, 1987a, 1988; Song and Viskanta, 1994) using $\mu_{\text{eff}} = \mu_{\text{f}}$ in the calculations.

2.3 Comparison of the velocity profiles

This short introduction to the state of the art in the field shows that the main features of interfacial momentum transport are rather well understood. But it should be noted that some fundamental issues concerning the correct formulation are still open and deserve some attention. In the two-domain approach, often presented as more rigorous, the solutions are in agreement with the experimental observations only after adjusting the *ad hoc* parameters α or β. Those parameters are said to depend on the structural characteristics of the porous interface, but no explicit relation has been provided so far. Also it is still not clear in which situations the continuity of the velocity associated to a stress jump condition (4) gives a better description than the models by Beavers and Joseph (1967) or Neale and Nader (1974). On the other hand, the single-domain approach remains questionable since the physical representation of momentum conservation in the interfacial region depends on how the effective properties of the porous medium spatially vary towards the thermophysical properties of the fluid phase porous medium and thus on the accuracy of the discretization scheme in the interfacial region.

The purpose of this section is not to completely answer the above questions, but to assess the general background of the problem formulation using the single- and the two-domain approaches. A detailed discussion including a description of the interface as a non-homogeneous medium is presented by Goyeau *et al.* (2003).

Here, we will just consider the basic configuration of the channel studied by BJ (Figure 1). The saturated porous region is homogeneous and the flow is assumed to be stationary and incompressible. Inertia effects in both regions are neglected. The two-domain model uses the Brinkman equation in the porous layer, and the Stokes flow in the fluid. If continuity is satisfied for shear stress and velocity at the fluid/porous interface (Neale and Nader, 1974), the dimensionless dynamic boundary conditions of the problem are given by:

$$u(1) = 0 \tag{7}$$

$$U(0) = u(0) \tag{8}$$

$$\left.\frac{\partial u}{\partial y}\right|_{y=0} = \alpha^2 \left.\frac{\partial U}{\partial y}\right|_{y=0} \tag{9}$$

$$U(-\hat{H}) = -Da\frac{\mathrm{d}P}{\mathrm{d}x} \tag{10}$$

where $Da = K/h^2$ is the Darcy number, K being the permeability of the porous layer, $\hat{H}$ its dimensionless thickness ($\hat{H} = H/h$) and $\alpha^2 = \mu_{\text{eff}}/\mu_{\text{f}}$. The analytical solution of

this two-domain model has been determined by Neale and Nader (1974). According to the above assumptions, the momentum transport equation (6) for the single-domain model also reduces to:

$$0 = -\frac{\mathrm{d}P}{\mathrm{d}x} - \frac{1}{Da}\,U + \alpha^2 \frac{\mathrm{d}^2 U}{\mathrm{d}y^2} \tag{11}$$

in the whole channel, where the Da and α values depend on the domain. The numerical approximation of this differential equation is based on a standard finite volume procedure. The numerical results presented hereafter are obtained using regular or irregular node distribution in the y-direction depending on the homogeneous character of the porous layer. The verification of the numerical model has been performed using the exact analytical solution of the Poiseuille flow when the porous wall is impermeable ($Da \rightarrow 0$).

The comparison between the numerical (Goyeau *et al.*, 2003) and analytical (Neale and Nader, 1974) results is presented in Table I which reports, for different Darcy numbers, the slip velocity $u(0)$ and the dimensionless thickness of the porous boundary layer:

$$\delta = \sqrt{Da}\ln\left(\left[\frac{50\big((1/Da) - 2\big)}{1 + (\alpha/\sqrt{Da})}\right]^{\alpha}\right). \tag{12}$$

The agreement is also illustrated by the velocity profiles shown in Figure 2. The reduced viscosity expression retained in the calculations, $\mu_{\mathrm{eff}}/\mu_{\mathrm{f}} = \varepsilon^{-1}$, is obtained from the Darcy-Brinkman model derivation using volume averaging (Whitaker, 1986; Quintard and Whitaker, 1994). Other expressions for the reduced viscosity have also been used and it is verified that the agreement with the analytical results does not depend on the particular expression of the reduced viscosity. These results confirm that the single-domain approach implicitly imposes shear stress continuity, as clearly shown in Figure 2. This good agreement is the basis on which we rely to justify the use of the one-domain approach in the studies on natural convection in such domains.

3. Vertical enclosures: flow structures and heat and mass transfer

One field of application of the issues discussed in Section 2 is the simulation of double diffusive convection taking place in a confined enclosure partially filled with a porous medium. Heat transfer and fluid flow through fibrous insulation (Lebreton *et al.*, 1991), natural convection heat and mass transfer in solidification (Beckermann *et al.*, 1988), or solute exchange in sediments in coastal environments (Webster *et al.*, 1996) are some

Darcy number	Analytical solution (Neale and Nader, 1974)		Numerical solution (Goyeau *et al.*, 2003)	
Da	$u(0)$	δ	$u(0)$	δ
1.02×10^{-1}	189.6	−1.610	189.5	−1.5954
4.50×10^{-2}	116.8	−1.218	116.73	−1.218
1.97×10^{-2}	72.70	−0.888	72.60	−0.888
1.10×10^{-2}	52.46	−0.704	52.38	−0.704
9.50×10^{-3}	48.38	−0.660	48.31	−0.663
6.70×10^{-3}	39.96	−0.575	39.88	−0.575
5.00×10^{-3}	34.10	−0.510	34.02	−0.509
2.68×10^{-3}	24.43	−0.390	24.30	−0.392

Table I. Comparison with the analytical solution for $K = 7.1 \times 10^{-9}\,\mathrm{m}^2$, $\varepsilon = 0.78$

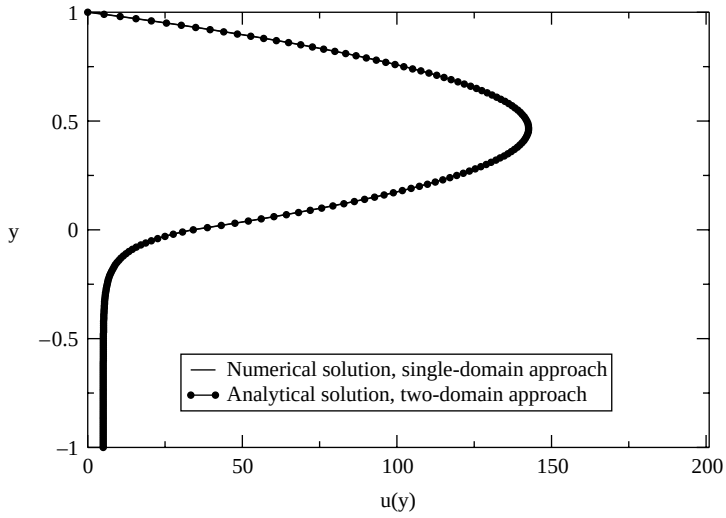

Figure 2.
Velocity profile: comparison between numerical (single-domain) and analytical (two-domain) solutions. $Da = 5 \times 10^{-3}$, $\varepsilon = 0.78$

Source: Goyeau *et al.* (2003)

examples of the fields where transport phenomena take place at an interface between a fluid phase and a porous medium. This is also relevant to a better understanding of convective heat and solute transfer in the mushy zone of a solidifying multi-component system, where natural convection is known to be driven by combined thermal and solutal buoyancy forces in the fluid phase. This particular class of natural convection with two buoyancy forces is also termed thermosolutal convection. We refer here to a simplified model where there is no phase change and where the dendritic region is represented as an homogeneous fixed porous medium.

It should first be noticed that very few experimental papers are available for such situations (Beavers and Joseph, 1967; Chen and Chen, 1989; Tachie *et al.*, 2003), and that the main effort has addressed the numerical simulation of such flows. The problem of thermal convection for such a configuration in a vertical enclosure where the porous layer is parallel to the vertical walls has been studied in the context of wall insulation (Arquis and Caltagirone, 1984; Sathe *et al.*, 1988; Lebreton *et al.*, 1991) or solidification (Beckermann *et al.*, 1987b, 1988; Song and Viskanta, 1994). An exact solution has been proposed by Weisman *et al.* (1999) and the stability problem has been tackled by Mercier *et al.* (2002). Numerical results for a vertical enclosure with two porous layers have been presented by Merrikh and Mohamad (2002). All these studies make use of the one-domain formulation.

Let us consider the simulation of double diffusive convective flows in a binary fluid, confined in a vertical enclosure, divided into two vertical domains, one porous layer and a fluid layer. Some studies are concerned with thermal insulation inside buildings, but the fluid under consideration is a gas-air mixture ($Pr = 0.7$) and the Lewis number is then on the usual order of magnitude for gases: $Le \sim \mathcal{O}(1)$. This considerably limits the interest of the results since the relevant features of double diffusion are related to high-Lewis numbers fluids ($Le \sim \mathcal{O}(10^2)$) for liquids or $Le \sim \mathcal{O}(10^4)$ for liquid metallic alloys). We will analyze some specific features of double diffusive convection in such a partially

porous enclosure, emphasizing the influence of the characteristics of the porous layer and the separate role of the double diffusive parameters.

3.1 Mathematical formulation

The geometry under consideration is the 2D rectangular cavity (height – H, total width – L) shown in Figure 3, where the porous layer (thickness x_P^*) along the left wall is assumed to be homogeneous and isotropic. The porous medium is saturated by the binary fluid which fills the remaining of the enclosure. Different uniform temperatures and concentrations are specified at the external vertical walls of the cavity, and zero heat and species fluxes are assumed at the horizontal boundaries. The flow is assumed to be laminar and incompressible, and the binary fluid to be Newtonian and to satisfy the linear Boussinesq approximation:

$$\rho = \rho_0[1 - \beta_T(T - T_0) - \beta_C(C - C_0)] \tag{13}$$

Moreover, the porous matrix is supposed to be in thermal equilibrium with the fluid, and the Soret and Dufour effects are neglected. The mathematical model results from the coupled system of conservation equations derived from the one-domain approach presented above, which considers the porous layer as a pseudo-fluid and the composite region as a continuum, which leads to solve only one set of coupled equations. Under the foregoing hypotheses, the macroscopic conservation equations both retain the Darcy-Brinkman formulation in the porous layer and the Navier-Stokes equation in the binary fluid, the expression of the permeability being a prescribed function of space. In terms of the dimensionless variables defined in the nomenclature, the steady state macroscopic conservation equations resulting from the present model are written:

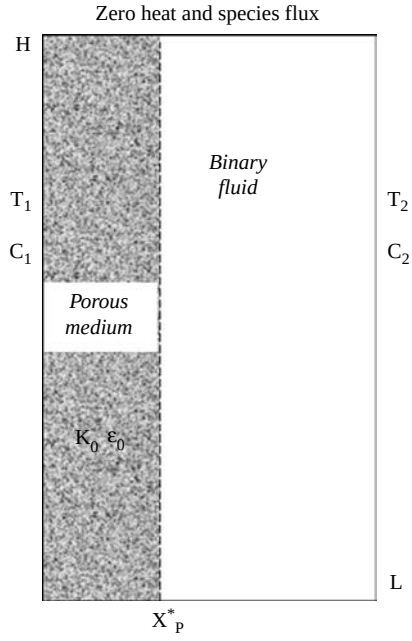

Figure 3.
Schematic description of the problem

$$\nabla . V = 0 \tag{14}$$

$$\frac{1}{\varepsilon^2 Pr}(V.\nabla)V = -\frac{\nabla P}{Pr} + Ra_T(\theta + N\phi)k - \frac{1}{Da}V + \frac{\mu_{eff}}{\mu_f}\nabla^2 V \tag{15}$$

$$V.\nabla\theta = \frac{k_{eff}}{k_f}\nabla^2\theta \tag{16}$$

$$V.\nabla\phi = \frac{1}{Le}\frac{\mathscr{D}_{eff}}{\mathscr{D}}\nabla^2\phi \tag{17}$$

At the boundaries, zero heat or species flux conditions are prescribed at the horizontal walls and Dirichlet boundary conditions at the vertical walls: $\theta = \phi = -0.5$ at the porous medium external wall ($x = 0$) and $\theta = \phi = 0.5$ at the vertical wall in contact with the fluid ($x = 1/A$).

The problem is characterized by the set of dimensionless parameters generally defined for double diffusive convection in fluids, plus the parameters characterizing porous media:

- the thermal Rayleigh number defined with the fluid properties, Ra_T;
- the buoyancy ratio $N = \beta_C \Delta C / \beta_T \Delta T$;
- the Prandtl and Lewis numbers of the fluid, Pr and Le;
- the Darcy number (dimensionless permeability) of the porous layer, Da; and
- geometrical parameters, the aspect ratio of the enclosure A, and the reduced thickness of the porous layer, $x_P = x_P^*/L$.

μ_f, k_f and $\mathscr{D}_f$ refer to the dynamic fluid viscosity, thermal conductivity and molecular diffusivity, respectively, while subscript "eff" refers to the corresponding effective properties of the porous medium. The Nusselt and Sherwood numbers are the dimensionless average heat and mass fluxes along the vertical walls.

The set of equations (14)-(17) is numerically solved using a standard finite volume procedure. The detailed description of the method may be found elsewhere (Gobin *et al.*, 1998) and only specific features of the method are recalled hereafter. The method has been successfully used by the authors to solve heat and fluid flow problems in fluids and porous media in similar ranges of parameters. It has been first verified that thermal and thermosolutal natural convection results for $x_P \rightarrow 1$ at any value of the Da number were in agreement with the standard Darcy-Brinkman version of the code and it has checked that at high values of the Darcy number the results at any value of x_P were identical to the results obtained for the pure fluid problem. The calculations in the non-homogeneous cavity have been compared for thermal convection against the existing results (Lebreton *et al.*, 1991). Depending on the permeability of the fluid layer, the strong temperature, concentration or velocity gradients may be located in the vicinity of the fluid-porous interface. Consequently, for low-permeabilities compound meshes are used in order to limit the computational cost, and two distinct irregular (generally sinusoidal) horizontal grids are taken in the porous layer and in the fluid cavity. The number of nodes in each domain is a function of the Rayleigh numbers and of the thickness of the porous region. Typical values range between 145 and 252 nodes for the x-direction and from 202 up to 402 regularly spaced nodes in the z-direction, in order to solve the multicellular structures.

3.2 Influence of the porous layer thickness and permeability

The results presented here concern a standard reference configuration ($Ra_T = 10^6$, $N = 10$, $Pr = 10$, $Le = 100$, $A = 2$). As can be seen from the results displayed in Figure 4 showing the variation of the Sherwood number for a given permeability of the porous domain ($Da = 10^{-5}$), the thickness of the porous layer has a significant influence on mass transfer in the enclosure, even for small values of x_P. This influence is seen to be limited here to $x_P < 0.1$, since for thicker porous layers (between 0.20 and 0.9) the Sherwood number is not very sensitive to x_P.

The variation of the average mass transfer as a function of the Darcy number for different values of the porous layer thickness (Figure 5) shows that when the permeability of the porous layer increases from very low values ($Da \sim 10^{-9}$) to high values corresponding to a fluid ($Da \sim 1$), the Sherwood number is continuously increasing. A second feature is that, compared to the pure fluid cavity ($x_P = 0$, represented here by the result at $Da = 1$), the influence of the porous layer thickness on the mass transfer decrease is essentially noticeable in the low-permeability range ($Da < 10^{-6}$). In this range, the comments made on Figure 4 apply for different values of the Darcy number. At higher permeabilities, the presence of the porous layer induces a drastic decrease of the Sherwood number even for a small thickness ($x_P = 0.1$) of the porous layer, but there is almost no sensitivity to x_P. If we now consider the evolution of the average heat transfer with the same variations of Da and $x_P = 0.1$ (Figure 6), the first observation is that this evolution is no longer monotonous. The second observation is the strong sensitivity of the heat transfer characteristics to the porous layer thickness at all permeabilities in the [0.1-0.8] range. Note that for thick porous layers ($x_P > 0.8$) the average Nusselt number remains very close to the pure conduction limit ($Nu = A = 2$) over a wide range of Darcy numbers, indicating the absence of convective heat transfer in this range. This shows that the effect of the porous layer thickness on the boundary layers is not the same for species

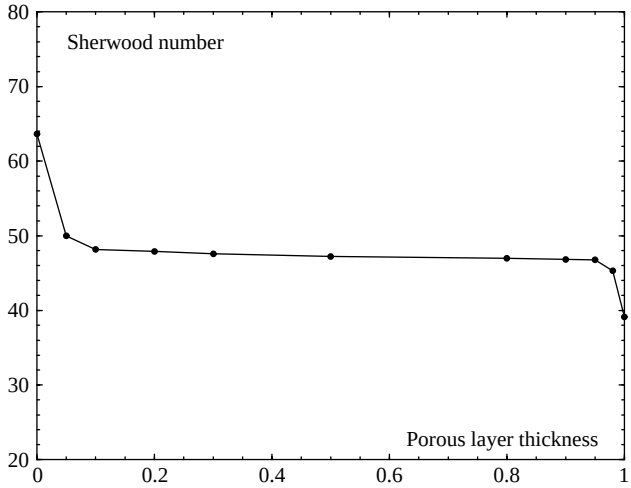

Source: Gobin *et al.* (2005)

Figure 4.
Average mass transfer variation as a function of the porous layer thickness at $Da = 10^{-5}$, $Ra_T = 10^6$, $N = 10$, $Le = 100$, $Pr = 10$, $A = 2$

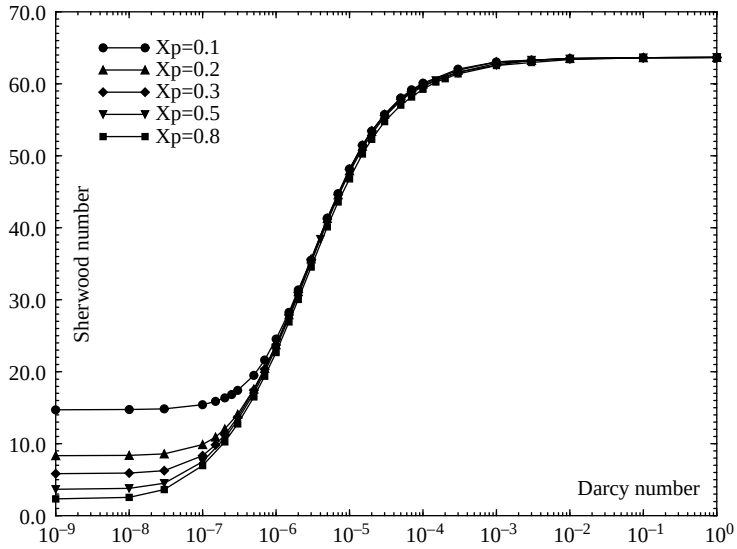

Source: Gobin *et al.* (2005)

Figure 5.
Mass transfer variation with permeability for different porous layer thicknesses at $Ra_T = 10^6$, $N = 10$, $Pr = 10$, $A = 2$

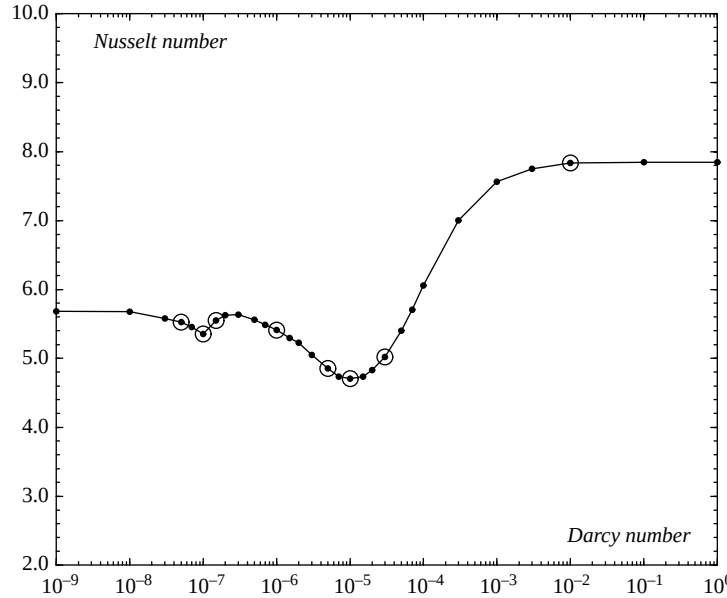

Figure 6.
Heat transfer variation for the reference case ($x_P = 0.1$)

distribution and for the thermal field: we can show that this is due to the difference in diffusion lengths for θ and ϕ and thus to the Lewis number.

In this section the analysis of the results is presented for the standard reference configuration defined above ($Ra_T = 10^6, N = 10, Pr = 10, Le = 100, A = 2$) and $x_P = 0.1$. The evolution of the convective flow with increasing permeability results from the competition between two opposing effects. First, the higher permeability results in a better penetration of the porous layer by the flow and consequently the diffusive damping of the imposed temperature and concentration difference in the layer is smaller. The effective temperature and composition gradients governing the buoyancy forces is then expected to grow and the flow to be accelerated, resulting in higher heat and mass transfer. This is what may be observed on the Sherwood number. On the other hand, due to the difference between the thermal and molecular diffusivities, the central recirculation loop driven on the scale of the thermal boundary layer thickness is driven by a relatively smaller temperature difference. Locally the ratio of the buoyancy forces decreases and the intensity of the internal thermal loop is decreasing, and also the average heat transfer. The double diffusive process is thus dominating the evolution. The foregoing analysis is intended to refine the interpretation of this behavior in terms of the thermosolutal features of the solution. First, when displaying the streamlines at different values of the Darcy number, it is clearly seen (Figure 7) that the existence of a minimum is directly related to the flow structure. In the neighborhood of the first minimum, one may observe that the decrease in the Nusselt number is caused by a decrease of the main recirculation cell, due to the formation of a low-velocity zone in the bottom part of the enclosure where the heat transfer is mainly conductive. This "stagnant" zone is compositionally stratified as in typical double diffusive problems (Gobin and Bennacer, 1996), while the heat transfer in this region is mainly conductive. With the increasing height of the stagnant zone, the local vertical concentration gradient decreases and gets destabilized by the lateral temperature gradient, resulting in the formation of a secondary co-rotative cell and a sudden increase of the Nusselt number. Then the formation process of a stagnant zone at the bottom of the enclosure resumes at $Da \sim 2 \times 10^{-7}$ with the related decrease in heat transfer, until the development of a third recirculation cell allows for a new enhancement of the average heat transfer (Figure 7). Then, the increase in Darcy number results in a better penetration of the porous layer by the flow, until, at very high permeabilities a fully symmetrical tri-cellular structure characteristic of double diffusion in liquids is recovered.

3.3 Influence of the double diffusive parameters

As mentioned earlier, the specific features of double diffusive convection appear when the characteristic diffusion lengths for heat and solute are different. The parameter

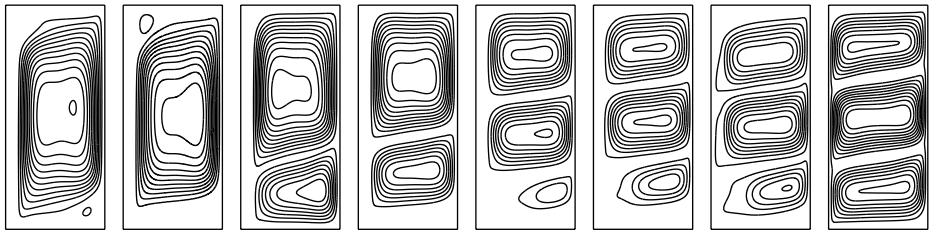

Figure 7.
Reference case – flow structure ($\Delta\Psi = 0.1$, $Ra_T = 10^6$, $N = 10$, $x_P = 0.1$, $Le = 100$, $Pr = 10$, $A = 2$)

which governs the ratio between thermal and molecular diffusivity (the Lewis number) is currently on the order of 10^2 or more, except for gases where $Le \sim 1$. In the latter case, the scale of heat and solute boundary layers are similar and the buoyancy forces have a merely additive effect. No multicellular structure is expected and the dependence of the Nusselt number with permeability follows the same variation as the Sherwood number, a smoothly monotonous increase, as shown in Figure 5. In this section, we first study the influence of the Lewis number: even if the low and moderate values of Le are not realistic, the comparison is intended to show its influence on the heat and mass transfer characteristics. All the parameters are fixed, except for the mass diffusivity, meaning that the solutal Rayleigh number is increased in the same proportion as the Lewis number. The Sherwood number is uniformly increased with Le (not shown) and we see (Figure 8) that the Nusselt number variation is similar at low values ($Le \leq 5$), and the heat transfer is decreasing as Le increases, as expected from the scaling laws in the solutally dominated regime ($N > 1$) (Bejan, 1985). The Nusselt curve shows only one minimum for $Le = 10$. It could be shown that the flow structure remains monocellular but the mechanism is similar to the second minimum of the reference case described above and the decrease in heat transfer is compensated around $Da = 3 \times 10^{-5}$ by the penetration of the porous layer.

The other interesting feature to be analyzed is the influence of the buoyancy ratio. It is also well known that the double diffusive features of the flow are of mostly visible in the intermediate regime between the heat transfer dominated ($N \ll 1$) and the mass transfer dominated $N > > 1$) regimes, where both buoyancy forces are in competition. The numerical results presented here concern positive values of N ranging from 1 to 10 for the same set of parameters, including $Le = 100$ (Figure 9). Again the Sherwood number (not shown) has the same qualitative behavior at different values of N except that the increase in mass transfer occurs at smaller Da for higher N. If we consider the

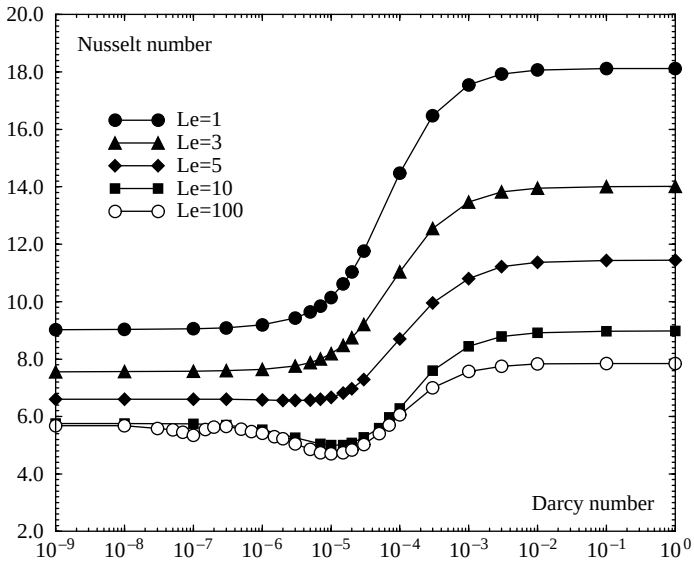

Source: Gobin *et al.* (2005)

Figure 8.
Heat transfer variation with permeability for different Lewis numbers at $N = 10$, $Ra_T = 10^6$, $Pr = 10$, $A = 2$, $x_P = 0.1$

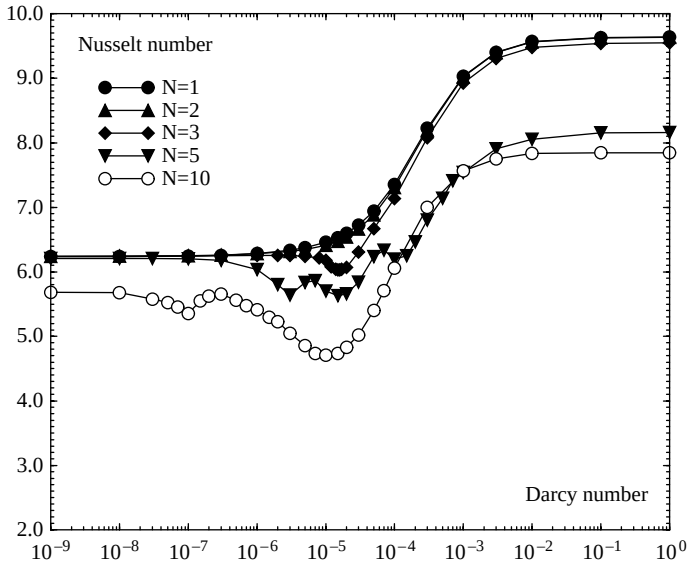

Source: Gobin *et al.* (2005)

Figure 9.
Heat transfer variation with permeability for different buoyancy ratios at $Le = 100$, $Ra_T = 10^6$, $Pr = 10$, $A = 2$, $x_P = 0.1$

Nu curves (Figure 9), there is almost no difference between $\beta_C \Delta C / \beta_T \Delta T = 1$ or 2, for which the Nusselt number variation is monotonous. A minimum may be noticed at $N = 3$, but the limiting values (at $Da < 10^{-7}$ or $Da < 10^{-3}$) are also identical: here only the solutal Rayleigh number is modified through N and it is known to have little influence on the Nusselt number. At $N = 3$, one could show that the flow structure remains monocellular, a stagnant zone is formed at the bottom of the enclosure in the intermediate range of permeabilities, which results in a decrease of the average heat transfer. In this particular situation this zone remains stable, because the flow penetration of the porous layer accelerates the fluid before the stratified zone gets destabilized. For $N = 5$, the flow structure exhibits three minima:

- the first minimum corresponds to the formation of a second cell;
- in the neighborhood of $Da = 10^{-5}$ a stagnant zone is formed below the second cell but this zone does not reach destabilization and the second cell increases again;
- around $Da = 10^{-4}$ the flow penetration progressively increases the strength of the first cell and the second cell finally disappears; and
- at high permeabilities the flow is mono-cellular.

The $N = 5$ curve shows the transition between a globally monocellular flow structure at $N \leq 3$ and the three-cell structure at $N = 10$.

As a conclusion to this section, it can be shown that the influence of a thin porous layer on the side of a rectangular enclosure has a remarkable influence on the heat and mass transfer characteristics. Even if the conditions are significantly different from those met in solidification processes, it seems to be important to carefully analyze those features to understand the coupling between double diffusive convection and the dynamics of solidification.

4. Natural convection in superposed horizontal layers: the stability problem

A different class of problems combining adjacent fluid and porous layers deals with natural convection in horizontal systems. The problem is relevant for instance to the stability of solidification of a horizontal layer cooled from below. Although the classical Rayleigh-Bénard problem in horizontal fluid or porous layers has been extensively studied in the literature, there are relatively few studies concerning composite domains. Here, our interest addresses the stability of the diffusive base solution in a two layer system consisting of a horizontal fluid layer overlying a porous layer. In this case again the coupling of the Navier-Stokes equation with the Darcy's law (or one of its extensions) through an appropriate set of boundary conditions at the fluid/porous interface is of interest. The first study in this field is due to Chen and Chen (1988) who have shown that the marginal stability curves, i.e. the critical Rayleigh number against the wave number curves, exhibit two possible regimes. Carr and Straughan (2003) have considered the same two-layer system, with a stress free boundary condition at the upper surface. To simulate penetrative convection for water, they have adopted an equation of state which expresses the density in the buoyancy force as a quadratic function of temperature. Carr (2004) made an important extension to this work, considering penetrative convection via internal heating. In spite of the difference in the physical quantities driving the motion between these two studies, the results also exhibit the bimodal nature of the solution. The alternative to the two domain description has been developed by Zhao and Chen (2001) using the one domain approach. They could capture the bimodal characteristics of the stability curves, but the values obtained with this latter model were about 30-40 percent smaller than the critical values assessed in Chen and Chen (1988), reactivating the interest for the comparison of the two formulations.

4.1 Problem formulation

Here, we use the two-domain formulation of the problem for the linear stability analysis of thermal natural convection in superposed fluid and porous layers. Note that if one wishes to handle spatial property variations (for example, evolving heterogeneities) the one-domain formulation may be preferred (Hirata *et al.*, 2006). The system under consideration consists of a horizontal porous layer of thickness d_{m}^{*} underlying a fluid layer of thickness d_{f}^{*}, with a total thickness $d^{*} = d_{\mathrm{m}}^{*} + d_{\mathrm{f}}^{*}$. The upper and lower walls are considered impermeable and are kept at temperatures T_{u}^{*} and T_{l}^{*}, respectively. The porous medium is saturated by the same fluid which fills the rest of the domain, and is supposed to be in thermal equilibrium with the fluid. Finally, the fluid is assumed to be Newtonian and to satisfy the Boussinesq approximation and the porous medium is supposed to be isotropic and homogeneous. The dimensionless governing equations are written separately for the porous layer ($0 < y^{*} < d_{\mathrm{m}}^{*}$) and for the fluid region ($d_{\mathrm{m}}^{*} < y^{*} < d^{*}$). When the Darcy-Brinkman formulation is retained the effective viscosity μ_{eff} is such that $\mu_{\mathrm{eff}}/\mu = 1/\varepsilon$ (Whitaker, 1999).

The boundary conditions at the upper and lower boundaries are the imposed temperatures and zero velocities. At the interface $y^{*} = d_{\mathrm{m}}^{*}$, continuity of temperature, heat flux, velocity, normal stress and tangential stress are imposed:

$$T^{*} = T_{\mathrm{m}}^{*} \tag{18}$$

$$k_{\mathrm{f}} \frac{\partial T^{*}}{\partial y^{*}} = k_{\mathrm{m}} \frac{\partial T_{\mathrm{m}}^{*}}{\partial y^{*}} \tag{19}$$

$$V^* = V_{\mathrm{m}}^* \tag{20}$$

$$-P^* + 2\mu \frac{\partial w^*}{\partial y^*} = -P_{\mathrm{m}}^* + 2\mu_{\mathrm{eff}} \frac{\partial w_{\mathrm{m}}^*}{\partial y^*} \tag{21}$$

$$\mu \frac{\partial u^*}{\partial y^*} = \mu_{\mathrm{eff}} \frac{\partial u_{\mathrm{m}}^*}{\partial y^*} \tag{22}$$

It is important to note that, when using the Darcy equation, the continuity of normal stress does not include the viscous contribution in the porous region, and the continuity of tangential stress is substituted by the BJ boundary condition (equation (1)).

In order to derive the perturbation equations, we impose perturbations to the basic solution of the dependent variables:

$$\xi = \bar{\xi}(y) + \xi'(x, y, t) \tag{23}$$

where the overlined quantities represent the basic state and the primes denote the perturbation profiles. The steady basic state is supposed to be quiescent: $\bar{V} = 0$ and $\partial/\partial t = 0$. The equations are linearized in the usual manner. After some manipulations and eliminating pressure, the perturbation equations are:

(1) For the fluid layer:

$$\left(\frac{\partial}{\partial t} - \nabla^2\right) \nabla^2 w' = Gr_{\mathrm{T}} \nabla_2^2 \theta' \tag{24}$$

where $\nabla_2^2 = \partial^2/\partial x^2$ in 2D and $\nabla_2^2 = \partial^2/\partial x^2 + \partial^2/\partial z^2$ in three dimensions:

$$\frac{\partial \theta'}{\partial t} + \frac{\partial \bar{\theta}}{\partial y} w' = \frac{1}{Pr_{\mathrm{f}}} \nabla^2 \theta' \tag{25}$$

(2) For the porous layer:

$$\left(\frac{1}{\phi} \frac{\partial}{\partial t} - \eta \nabla^2\right) \nabla^2 w' m + \frac{1}{Da} \nabla^2 w_m' = Gr_{\mathrm{T}} \nabla_2^2 \theta_{\mathrm{m}}' \tag{26}$$

$$\frac{(\rho_0 C_{\mathrm{P}})_{\mathrm{m}}}{(\rho_0 C_{\mathrm{P}})_{\mathrm{f}}} \frac{\partial \theta_{\mathrm{m}}'}{\partial t} + \frac{\partial \bar{\theta}_{\mathrm{m}}}{\partial y} w_m' = \frac{1}{Pr_{\mathrm{m}}} \nabla^2 \theta_{\mathrm{m}}' \tag{27}$$

Applying the normal mode analysis to the dependent variables, we assume:

$$(w', \theta') = (W(y), \Theta(y)) f(x) e^{i\kappa y + \sigma t} \tag{28}$$

where $W(y)$ and $\Theta(y)$ are the amplitude of the velocity and temperature, respectively. κ is the dimensionless horizontal wave number and σ is the complex growth rate. We assume that the principle of exchange of instabilities holds, and the onset of instability is in the form of steady convection ($\sigma = 0$). Substituting equation (28) in equation (24)-(27), we obtain:

$$\frac{\mathrm{d}^4 W}{\mathrm{d}y^4} - 2\kappa^2 \frac{\mathrm{d}^2 W}{\mathrm{d}y^2} + \kappa^4 W = \kappa^2 Gr_{\mathrm{T}} \Theta \tag{29}$$

$$\frac{d^2\Theta}{dy^2} - \kappa^2\Theta = \frac{1+\hat{d}}{\hat{d}+\varepsilon_T} Pr_f W \tag{30}$$

$$\eta\frac{d^4 W_m}{dy^4} - \left(2\eta\kappa^2 + \frac{1}{Da}\right)\frac{d^2 W_m}{dy^2} + \left(\eta\kappa^4 + \kappa^2\frac{1}{Da}\right) W_m = \kappa^2 Gr_T \Theta_m \tag{31}$$

$$\frac{d^2\Theta_m}{dy^2} - \kappa^2\Theta_m = \varepsilon_T\frac{1+\hat{d}}{\hat{d}+\varepsilon_T} Pr_m W_m \tag{32}$$

with $\eta = \mu_{eff}/\mu_f$.

At the interface, the continuity conditions are as follows:

$$\Theta = \Theta_m \tag{33}$$

$$\frac{d\Theta}{dy} = \frac{1}{\varepsilon_T}\frac{d\Theta_m}{dy} \tag{34}$$

$$W = W_m \tag{35}$$

$$\frac{dW}{dy} = \frac{dW_m}{dy} \tag{36}$$

$$-\frac{d^3 W}{dy^3} + 3\kappa^2\frac{dW}{dz} = \frac{1}{Da}\frac{dW_m}{dy} - \eta\left(\frac{d^3 W_m}{dy^3} - 3\kappa^2\frac{dW_m}{dy}\right) \tag{37}$$

$$\frac{d^2 W}{dy^2} = \eta\frac{d^2 W_m}{dy^2}. \tag{38}$$

A hybrid numerical-analytical solution for the eigenvalue problem resulting from the stability analysis is proposed. The original set of coupled partial differential equations is reduced into an infinite system of ordinary differential equations, using the GITT method. This system is adequately truncated and numerically solved with Mathematica (Wolfram, 1991).

The method of analysis and the numerical code have been verified by comparison with the exact values for the limiting cases of the fluid Rayleigh-Bénard problem and for the porous layer case (Hirata *et al.*, 2007a). A similar procedure leads to the corresponding sets of equations if the Darcy formulation is used in the porous layer instead of the Darcy-Brinkman extension, or if the stress jump condition (4) is used at the interface instead of the continuity condition.

4.2 The bimodal stability curve

The analysis deals with the influence of the thickness ratio and of the dimensionless permeability of the porous layer (the Darcy number) on the stability of the system. Calculations are performed for a given value of the Prandtl number ($Pr = 10$), and in order to be consistent with previous works (Chen and Chen, 1988; Zhao and Chen, 2001), the marginal stability curves are presented in terms of the filtration Rayleigh number Ra_T^*.

As already observed by several authors, the marginal stability curve exhibits two possible modes depending on the values of the characteristic parameters. Figure 10 shows the bimodal nature of the stability curve obtained with the present two-domain

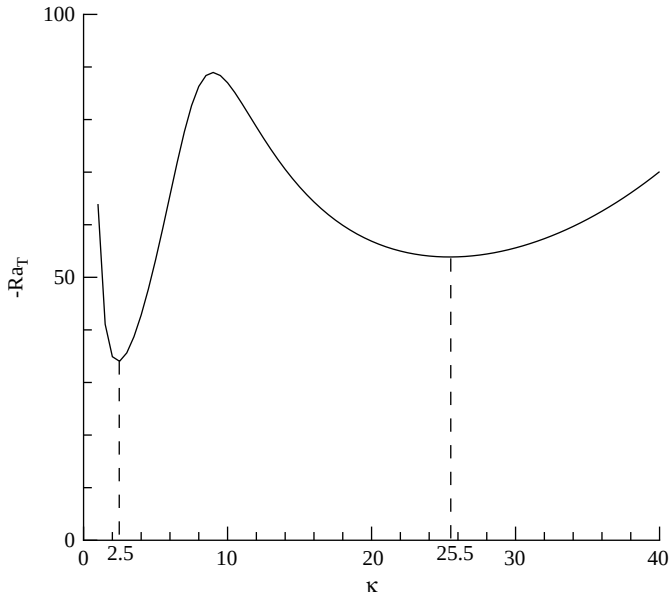

Figure 10.
Marginal stability curves for $\varepsilon_T = 0.7$ and $Da = 10^{-5}$ at $\hat{d} = 0.12$

Darcy-Brinkman model, for two values of the thickness ratio $\hat{d}$. The curve in Figure 10 ($\hat{d} = 0.12$) shows that the most unstable mode (minimum of the curve) is triggered for small wave number perturbations (here $\kappa = 2.5$), corresponding to a "porous" where the convective flow occurs in the entire porous region. For a slightly higher value of $\hat{d}$ (not shown) large wave number perturbations are more critical and lead to small wavelength cells, a "fluid" where the convective flow is mainly confined in the fluid layer. The two modes are illustrated by the streamline patterns obtained for $\kappa = 2.5$ and $\kappa = 25.5$, shown in Figures 11(a) and (b), respectively. The large wave number perturbation of results in small wavelength convection cells in the fluid layer with some flow penetration in the upper region of the porous layer, while the small wave number perturbation in case b affects the whole domain.

Concerning the influence of the Darcy number (not shown), it is found (Hirata *et al.*, 2006) that at large values of *Da* (very permeable media), the long-wave branch is the most unstable, and the onset of convective motion is produced in the porous medium. With decreasing permeability, flow penetration becomes more difficult and the short-wave branch becomes the most unstable. Under these conditions, convective cells develop within the fluid region.

4.3 Darcy vs. Darcy-Brinkman formulation

Figure 12 shows a comparison of the marginal stability curves obtained for the same value of the geometrical parameter that, using the present Darcy-Brinkman formulation and compared to the results obtained by Carr (2003) with the two-domain approach using the Darcy formulation for three different values of the adjustable slip coefficient α. Let us outline the relatively strong influence of the slip coefficient, since, in the selected example, the most unstable regime may depend on the α value. It may be observed that the stability curve obtained with the two-domain Darcy-Brinkman model

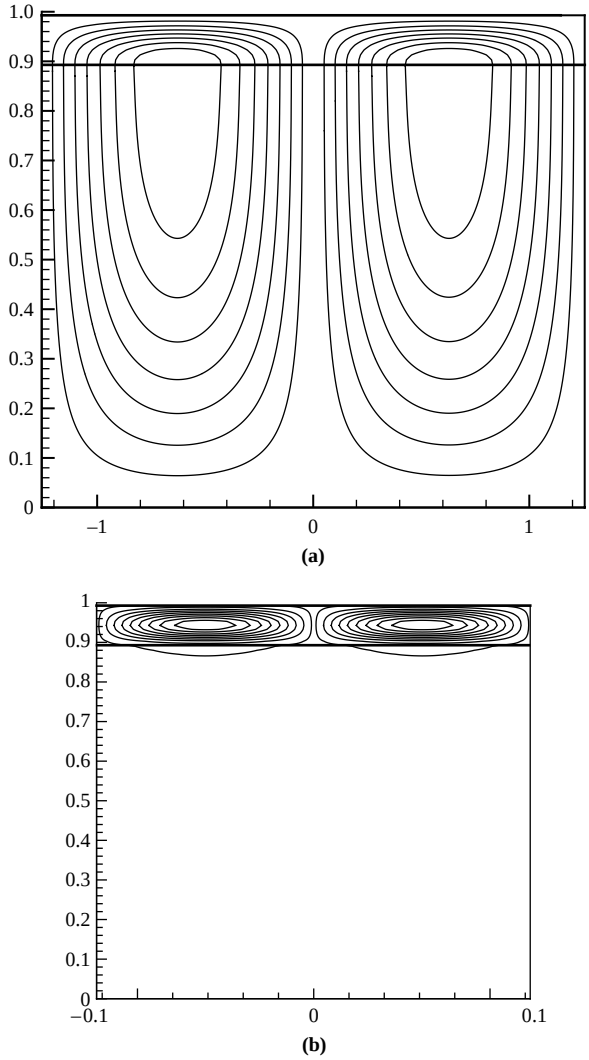

Figure 11.
Flow structure at the onset of convection for $\varepsilon_T = 0.7$ and $Da = 10^{-5}$

Notes: (a) $\widehat{d} = 0.12$, $\kappa = 2.5$; (b) $\widehat{d} = 0.12$, $\kappa = 25.5$ (the scale in the horizontal direction is not respected

(no adjustable parameter) is located between the curves given by the Darcy model for $\alpha = 1$ and $\alpha = 4$. This result is fully consistent with the fact that the BJ condition and the Neale and Nader model are compatible for $\alpha^2 = \mu_{\text{eff}}/\mu = 1/\varepsilon$. Here, $\varepsilon = 0.39$, corresponding to $\alpha = 1.6$, which is in the correct range. This comparison shows the superiority of the Brinkman extension to Darcy's law, which does not require the use of any adjustable parameter.

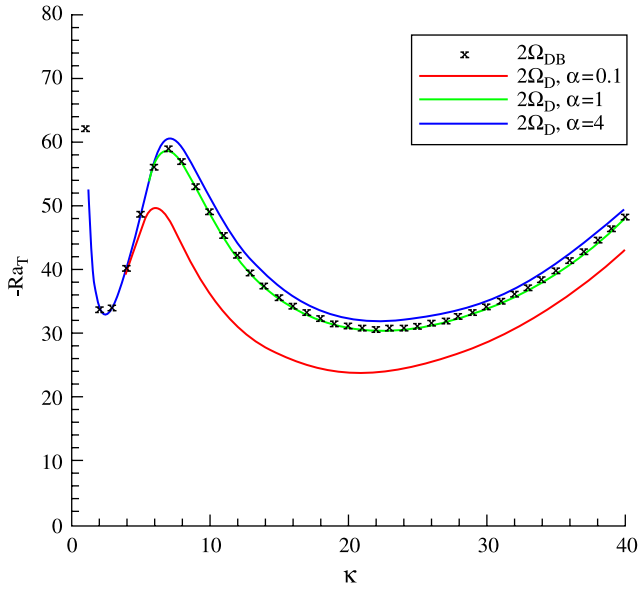

Figure 12.
Marginal stability curves – comparison of the Darcy ($\alpha = 0.1$, 1 and 4) and of the Darcy-Brinkman models

The comparison between the results given by the one-domain model and the two-domain formulation is still to be completed. Preliminary results show that the quality of the results may depend on the rate of variation of the properties at the transition between the fluid and the porous layer, and the accuracy of the numerical approximation in this area has to be carefully verified.

4.4 The stress jump condition

As we have seen in Section 2, the two-domain formulation may account for a non-homogeneous region in the vicinity of the interface. The integral form of this permeability variation may be represented by the stress jump condition at the interface proposed by Ochoa-Tapia and Whitaker (1995a) as equation (4). As α in the BJ condition, the parameter β in this equation describes the structure of the fluid-porous interface. Comparing with the BJ experiments, Ochoa-Tapia and Whitaker (1995b) have shown that the value of β is on the order of 1. ($\beta = 0$ meaning continuity of the shear stress).

It is interesting to introduce this new condition in the analysis, and to see the influence of the β value on the stability limit (Hirata *et al.*, 2007b). This is shown in Figure 13 of the filtration Rayleigh number for $\hat{d} = 0.10$, $Da = 10^{-5}$ and $\varepsilon = 0.39$. As expected, the bimodal nature of the stability curve is obtained, each mode corresponding to a different mode of convective instability. The figure shows that with a larger stress jump coefficient the fluid mode is strongly modified, and the stability limit is decreases at large wave numbers, while the porous mode remains unsensitive to the β value. This may be explained considering that the spatial variation of the permeability in the interfacial region through the jump condition (4) leads to an increase of the interface velocity.

The influence of β for different values of the Darcy number is shown in Figure 14. For small or for very large values of the dimensionless bulk permeability *Da*, the stress

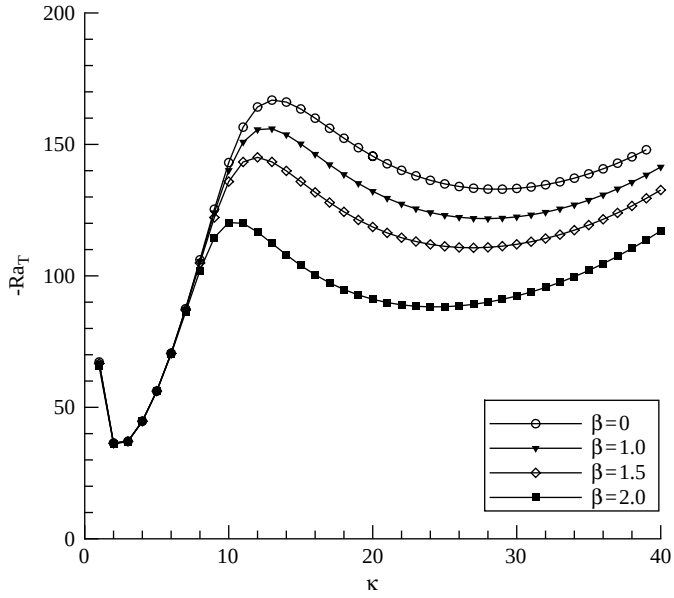

Figure 13.
Influence of the stress jump coefficient β for $\hat{d} = 0.10$, $Da = 10^{-5}$ and $\varepsilon = 0.39$

Source: Hirata *et al.* (2007b)

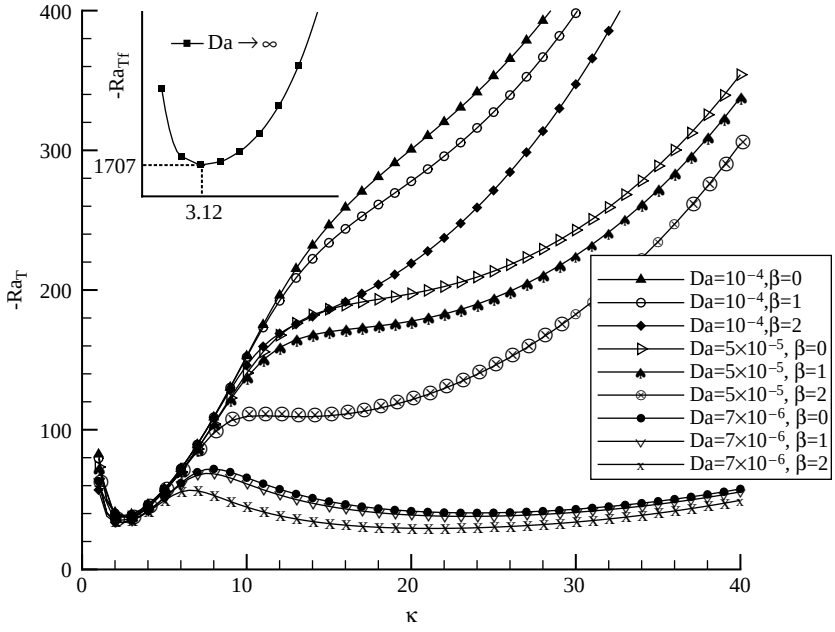

Figure 14.
Influence of the stress jump coefficient β for different Darcy numbers at $\hat{d} = 0.14$

Source: Hirata *et al.* (2007b)

coefficient has little influence on the marginal stability curves. In these limiting cases, the porous layer either tends towards a solid wall (small *Da*) and a no-slip condition holds at the interface, or the porous media behaves as a fluid (large *Da* numbers) and the interface disappears. For intermediate values of the Darcy number, it may be observed that the influence of the jump coefficient on the marginal stability curves may be significant. These results clearly illustrate the importance of the fluid-porous interfacial modelling. This is particularly true for very irregular interfaces, where the complexity of the microstructure has to be taken into account.

5. Conclusion

This brief overview on the heat and mass transfer problems with fluid flow in domains filled with pure or binary fluids and including a porous partition (superposed layers and composite cavities) shows that new features either in terms of stability limits or in terms of heat and mass transfer characteristics and flow structures may be studied.

The problem of the single- vs two-domain formulation has been discussed. It seems that, provided sufficient care is taken in the numerical approximations, both approaches lead to similar results for the simulation of heat and fluid flow in fluid-porous domains. Concerning the stability studies more work is requested to verify this statement. This is still in the field of current research.

References

Adler, P.M. (1978), "Viscosity of concentrated suspensions of aggregable particles", *Rheol. Acta.*, Vol. 17, pp. 288-95.

Arquis, E. and Caltagirone, J-P. (1984), "Sur les conditions hydrodynamiques au voisinage d'une interface milieu fluide-milieu poreux: application à la convection naturelle", *C.R. Acad. Sciences Paris*, Vol. 299 No. 1, pp. 1-4.

Bear, J. and Bachmat, Y. (1990), *Introduction to Modeling of Transport Phenomena in Porous Media*, Kluwer Academic, Norwell, MA.

Beavers, G.S. and Joseph, D.D. (1967), "Boundary conditions at a naturally permeable wall", *J. Fluid Mech.*, Vol. 30 No. 1, pp. 197-207.

Beavers, G.S., Sparrow, E.M. and Magnuson, R.A. (1970), "Experiments on coupled parallel flows in a channel and a bounding porous medium", *J. of Basic Engineering*, Vol. 92, pp. 843-8.

Beavers, G.S., Sparrow, E.M. and Masha, B.A. (1974), "Boundary condition at a porous surface which bounds a fluid flow", *AIChe J.*, Vol. 20 No. 3, pp. 596-7.

Beckermann, C., Ramadhyani, S. and Viskanta, R. (1987a), "Natural convection flow and heat transfer between a fluid layer and a porous layer inside a rectangular enclosure", *ASME J. Heat Transfer*, Vol. 109, pp. 363-70.

Beckermann, C., Ramadhyani, S. and Viskanta, R. (1987b), "Natural convection flow and heat transfer between a fluid layer and a porous layer inside a rectangular enclosure", *J. Heat Transfer*, Vol. 109, pp. 363-70.

Beckermann, C., Viskanta, R. and Ramadhyani, S. (1988), "Natural convection in vertical enclosures containing simultaneously fluid and porous layers", *J. Fluid Mech*, Vol. 186, pp. 257-84.

Bejan, A. (1985), "Mass and heat transfer by natural convection in a vertical cavity", *Int. J. Heat Fluid Flow*, Vol. 6 No. 3, pp. 149-59.

Brinkman, H.C. (1947), "A calculation of the viscous force exerted by flowing fluid on a dense swarm of particles", *Appl. Sci. Res.*, Vol. A1, pp. 27-34.

Carr, M. (2003), "A model for convection in the evolution of under-ice melt ponds", *Continuum Mechanics and Thermodynamics*, Vol. 15 No. 1, pp. 45-54.

Carr, M. (2004), "Penetrative convection in a superposed porous-medium-fluid layer via internal heating.", *J. Fluid Mech.*, Vol. 509, p. 305.

Carr, M. and Straughan, B. (2003), "Penetrative convection in a fluid overlying a porous layer", *Advances in Water Resources*, Vol. 26 No. 3, pp. 263-76.

Chen, F. and Chen, C.F. (1988), "Onset of finger convection in a horizontal porous layer underlying a fluid layer", *J. Heat Transfer*, Vol. 110, pp. 403-9.

Chen, F. and Chen, C.F. (1989), "Experimental investigation of convective stability in a superposed fluid and porous layer when heated from below", *J. Fluid Mech.*, Vol. 207, pp. 311-21.

Einstein, A. (1906), "Eine neue bestimmung der moleküldimensionen", *Annalen der Physik*, Vol. 19 No. 4, pp. 289-306, Trans. in 1956, Theory of the Brownian movement, Dover.

Ettefagh, J., Vafai, K. and Kim, S.J. (1991), "Non-Darcian effects in open-ended cavities filled with a porous medium", *ASME Journal of Heat Transfer*, Vol. 113, pp. 747-56.

Givler, R.C. and Altobelli, S.A. (1994), "Determination of the effective viscosity for the Brinkman-Forchheimer flow model", *J. Fluid Mech.*, Vol. 258, pp. 355-70.

Gobin, D. and Bennacer, R. (1996), "Cooperating thermosolutal convection in enclosures: 2. heat transfer and flow structure", *Int. J. Heat and Mass Transfer*, Vol. 39 No. 13, pp. 2683-97.

Gobin, D., Goyeau, B. and Neculae, A. (2005), "Convective heat and solute transfer in partially porous cavities", *Int. J. Heat Mass Transfer*, Vol. 48 No. 10, pp. 1898-908.

Gobin, D., Goyeau, D. and Songbe, J.P. (1998), "Double diffusive natural convection in a composite fluid-porous layer", *ASME J. Heat Transfer*, Vol. 120, pp. 234-42.

Goyeau, B., Lhuillier, D., Gobin, D. and Velarde, M. (2003), "Momentum transport at a fluid-porous interface", *Int. J. Heat Mass Transfer*, Vol. 46, pp. 4071-81.

Hirata, S.C., Goyeau, B. and Gobin, D. (2007b), "Stability of natural convection in superposed fluid and porous layers: influence of the interfacial jump boundary condition", *Phys. Fluids*, Vol. 19, pp. 4071-81.

Hirata, S.C., Goyeau, B., Gobin, D. and Cotta, R.M. (2006), "Stability of natural convection in superposed fluid and porous layers using integral transforms", *Num. Heat Transfer*, Vol. B-50, pp. 409-24.

Hirata, S.C., Goyeau, B., Gobin, D., Carr, M. and Cotta, R.M. (2007a), "Linear stability of natural convection in superposed fluid and porous layers: influence of the interfacial modelling", *Int. J. Heat Mass Transfer*, Vol. 50, pp. 1356-67.

Jäger, W. and Mikelić, A. (2000), "On the interface boundary condition of Beavers, Joseph, and Saffman", *SIAM J. Appl. Math.*, Vol. 60 No. 4, pp. 1111-27.

James, D.F. and Davis, A.M.J. (2001), "Flow at the interface of a model fibrous porous medium", *J. Fluid Mech.*, Vol. 426, pp. 47-72.

Joseph, D.D. and Tao, L.N. (1966), "Lubrification of a porous bearing-Stokes solution", *J. Appl. Mech.*, Vol. 33, pp. 753-60.

Kaviany, M. (1995), *Principles of Heat Transfer in Porous Media*, 2nd ed., Springer-Verlag, New York, NY.

Koplik, J., Levine, H. and Zee, A. (1983), "Viscosity renormalization in the Brinkman equation", *Phys. Fluids*, Vol. 26 No. 10, pp. 2864-70.

Kuznetsov, A.V. (1997), "Influence of the stress jump condition at the porous-medium/clear-fluid interface on a flow at a porous wall", *Int. C. Heat Mass Transfer*, Vol. 24 No. 3, pp. 401-10.

Kuznetsov, A.V. (1998), "Analytical investigation of Couette flow in a composite channel partially filled with a porous medium and partially with a clear fluid", *Int. J. Heat Mass Transfer*, Vol. 41 No. 16, pp. 2556-60.

Kuznetsov, A.V. and Ming-Xiong, M. (1999), "On the limitations of the single-domain approach for computation of convection in composite channels – comparisons with exact solutions", *Hybrid Methods in Engineering*, Vol. 1, pp. 249-64.

Larson, R.E. and Higdon, J.J.L. (1986), "Microscopic flow near the surface of two-dimensional porous media", *Part 1. Axial flow. J. Fluid Mech.*, Vol. 166, pp. 449-72.

Larson, R.E. and Higdon, J.J.L. (1987), "Microscopic flow near the surface of two-dimensional porous media", *Part 2. Transverse flow. J. Fluid Mech.*, Vol. 178, pp. 119-36.

Lebreton, P., Caltagirone, J.P. and Arquis, E. (1991), "Natural convection in a square cavity with thin porous layers on its vertical walls", *ASME J. Heat Transfer*, Vol. 113, pp. 892-8.

Levy, T. (1981), "Loi de Darcy ou loi de Brinkman", *C.R. Acad. Sciences*, Vol. 2 No. 292, pp. 871-4.

Lundgren, T.S. (1972), "Slow flow through stationary random beds and suspensions of spheres", *J. Fluid Mech.*, Vol. 51, pp. 273-99.

Martys, N., Bentz, D.P. and Garboczi, E.J. (1994), "Computer simulation study of the effective viscosity in Brinkman's equation", *Phys. Fluids*, Vol. 6 No. 4, pp. 1434-9.

Mercier, J.F., Weisman, C., Firdaous, M. and Le Quéré, P. (2002), "Heat transfer associated to natural convection flow in a partly porous cavity", *ASME J. Heat Transfer*, Vol. 124, pp. 130-43.

Merrikh, A.A. and Mohamad, A.A. (2002), "Non-darcy effect in buoyancy driven flows in an enclosure filled with vertically layered porous media", *Int. J. Heat Mass Transfer*, Vol. 45, pp. 4305-13.

Neale, G. and Nader, W. (1974), "Practical significance of Brinkman's extension of Darcy's law: coupled parallel flow within a channel and a bounding porous medium", *The Canadian J. of Chem. Eng.*, Vol. 52, pp. 475-8.

Nield, D.A. (1983), "The boundary correction for the Rayleigh-Darcy problem limitations of the Brinkman equation", *J. Fluid Mech.*, Vol. 128, pp. 37-46.

Nield, D.A. (1991), "The limitation of the Brinkman-Forchheimer equation in modeling flow in a saturated porous medium and at an interface", *Int. J. Heat and Fluid Flow*, Vol. 12 No. 3, pp. 269-72.

Nield, D.A. and Bejan, A. (2006), *Convection in Porous Media*, Springer, Berlin.

Ochoa-Tapia, J.A. and Whitaker, S. (1995a), "Momentum transfer at the boundary between a porous medium and homogeneous fluid -I. Theoretical development", *Int. J. Heat Mass Transfer*, Vol. 38 No. 14, pp. 2635-46.

Ochoa-Tapia, J.A. and Whitaker, S. (1995b), "Momentum transfer at the boundary between a porous medium and homogeneous fluid-II. Comparison with experiment", *Int. J. Heat Mass Transfer*, Vol. 38 No. 14, pp. 2647-55.

Quintard, M. and Whitaker, S. (1994), "Transport in ordered and disordered porous media III: closure and comparison between theory and experiment", *Transport in Porous Media*, Vol. 15, pp. 31-49.

Richardson, S. (1971), "A model for the boundary condition of a porous material. Part 2", *J. Fluid Mech.*, Vol. 49, pp. 327-36.

Saffman, P.G. (1971), "On the boundary condition at the surface of a porous medium", *Stud. Appl. Math.*, Vol. 50, pp. 93-101.

Sahraoui, M. and Kaviany, M. (1992), "Slip and no-slip velocity boundary conditions at interface of porous, plain media", *Int. J. Heat Mass Transfer*, Vol. 35 No. 4, pp. 927-43.

Saleh, S., Thovert, J.F. and Adler, P.M. (1993), "Flow along porous media by partical image velocimetry", *AICHE Journal*, Vol. 39 No. 11, pp. 1765-76.

Sathe, S.B., Lin, W.Q. and Tong, T.W. (1988), "Natural convection in enclosures containing an insulation with a permeable fluid-porous interface", *Int. J. Heat and Fluid Flow*, Vol. 9 No. 4, pp. 389-95.

Song, M. and Viskanta, R. (1994), "Natural convection flow and heat transfer within a rectangular enclosure containing a vertical porous layer", *Int. J. Heat Mass Transfer*, Vol. 37 No. 16, pp. 2425-38.

Starov, V.M. and Zhdanov, V.G. (2001), "Effective viscosity and permeability of porous media", *Colloids and Surfaces A: Physicochemical and Engineering Aspects*, Vol. 192, pp. 363-75.

Tachie, M.F., James, D.F. and Currie, I.G. (2003), "Velocity measurements of a shear flow penetrating a porous medium", *J. Fluid Mech.*, Vol. 493, pp. 319-43.

Taylor, G.I. (1971), "A model for the boundary condition of a porous material", *Part 1.J. Fluid Mech.*, Vol. 49, pp. 319-26.

Turki, S. and Lauriat, G. (1990), "An examination of two numerical procedures for natural convection in composites enclosures", *Proceedings of AIAA-ASME Thermophysics and Heat Transfer Conference, HTD*, Vol. 130, pp. 107-13.

Vafai, K. and Kim, S.J. (1990), "Fluid mechanics of the interface region between a porous medium and a fluid layer, an exact solution", *Int. J. Heat and Fluid Flow*, Vol. 11 No. 3, pp. 254-6.

Vafai, K. and Kim, S.J. (1995), "On the limitations of the Brinkman-Forchheimer-extended Darcy equation", *Int. J. Heat and Fluid Flow*, Vol. 16, pp. 11-15.

Webster, I.T., Norquay, S.J., Ross, F.C. and Wooding, R.A. (1996), "Solute exchange by convection within estuarine sediments", *Estuarine, Coastal and Shelf Science*, Vol. 42, pp. 171-83.

Weisman, C., Le Quéré, P. and Firdaouss, M. (1999), "Sur la solution exacte de la convection naturelle en cavité partiellement remplie d'un milieu poreux", *C.R. Acad. Sciences*, Vol. 327, pp. 235-40.

Whitaker, S. (1986), "Flow in porous media I: a theoretical derivation of Darcy's law", *Transport in Porous Media*, Vol. 1, pp. 3-35.

Whitaker, S. (1999), *The Method of Volume Averaging*, Vol. 13, Kluwer Academic, Norwell, MA.

Wolfram, S. (1991), *System for Doing Mathematics by Computer*, Addison-Wesley, Reading, MA.

Zhao, P. and Chen, C.F. (2001), "Stability analysis of double-diffusive convection in superposed fluid and porous layers using a one-equation model", *Int. J. Heat Mass Transfer*, Vol. 44, pp. 4625-33.

Corresponding author
Dominique Gobin can be contacted at: gobin@fast.u-psud.fr

To purchase reprints of this article please e-mail: **reprints@emeraldinsight.com**
Or visit our web site for further details: **www.emeraldinsight.com/reprints**